Raman probing of excited states of the tris(2,2′bipyridine)Cr(III) complex having lifetimes in the microand picosecond regions

M. Asano, J. A. Koningstein, and D. Nicollin

Citation: The Journal of Chemical Physics **73**, 688 (1980); doi: 10.1063/1.440170
View online: http://dx.doi.org/10.1063/1.440170
View Table of Contents: http://scitation.aip.org/content/aip/journal/jcp/73/2?ver=pdfcov
Published by the AIP Publishing

Raman probing of excited states of the tris(2,2'-bipyridine)Cr(III) complex having lifetimes in the micro-and picosecond regions[a)]

M. Asano, J. A. Koningstein, and D. Nicollin

Department of Chemistry, Carleton University, Ottawa K1S 5B6 Canada
(Received 18 January 1980; accepted 9 April 1980)

Population and Raman scattering of the ^2E and $^4T_2$ electronic excited states with lifetimes of $\tau_E \approx 60$ μs and $\tau_T \approx 10$ ps of the complex tris(2,2'-bipyridine)Cr(III) is achieved by exposing the complex $Cr(bpy)_3(ClO_4)_3$ in H_2O to radiation at 457.9 nm from tunable pulsed and cw fixed wavelength lasers. The spectra for ^2E and ground state $Cr(bpy)_3^{3+}$ are very similar but differences of intensities, FWHM and shifts of corresponding vibrational Raman bands of $^4T_2$ and $^4A_2$:$Cr(bpy)^{3+}$ are more pronounced. The differences in FWHM are attributed to the contribution to the overall Raman intensity for the former of vibrational scattering in vibrational states in the top as well as in the bottom of the $^4T_2$ electronic surface of some of the modes of the complex. This because the wavelength of the pumping source is in resonance with vibrational states in the top of that surface and the cascading process reveals itself in the time resolved Raman studies at the nanosecond level.

I. INTRODUCTION

The complex $Cr(bpy)_3^{3+}$ is of considerable interest because if dissolved [for example, the cation of a salt like $Cr(bpy)_3(ClO_4)_3$] in water, phosphorescence can be excited from an excited state ^2E having a lifetime of 30–60 μs.[1] This state can be readily populated and part of the absorption spectrum has been assigned to transitions which originate in this excited state.[1] Several studies[2–7] have also been made of the effect of the solvent on the lifetime of the ^2E metastable state of a number of polypyridyl complexes, and these studies included aspects of quenching and reactivity of the said state. In this paper, emphasis is placed on a relatively new spectroscopic technique which involves the excitation of Raman transitions of an optically pumped excited state and those induced for $Cr(bpy)^{3+}$ are vibrational in nature. Presently there are few reports in the literature[8–14] dealing with the subject of Raman transitions in high lying electronic states of ions in solids, molecules, or complexes. The results reported here are based on measurements with cw and pulsed lasers. From a practical point of view, it appears that the most convenient method which can be employed to obtain the light scattering spectrum in an excited state is that where part of the radiation of the cw or pulsed laser is used to produce the population, while Raman transitions are induced with that part of the radiation not used for population purposes.[8] The excited states of interest here are the ^2E at 13740 cm^{-1} and $^4T_2$ at $<17\,000$ cm^{-1}. The former is populated by pumping within the $^4T_2$ band system with ~50 mW at 457.9 nm of a cw laser, while the latter is populated using pulses with a duration of ~3.2 ns and a peak power of >100 kW of a N_2 pumped tunable dye laser operating in the spectral interval of 440–475 nm. The degree of population of these states can be determined from the dependence of the transmission[15] of the sample as a function of the laser power. The assignment of vibrational Raman transition in the electronic excited state is made following a comparison of the frequency and intensity spectrum including bandwidths as functions of the laser power. The former is discussed in Sec. II; the latter, in Sec. III of this communication.

II. POPULATION CHARACTERISTICS OF ^2E AND $^4T_2$ OF $Cr(bpy)_3^{3+}$

In this section we discuss the optical pumping processes for the compound $Cr(bipyridine)_3(ClO_4)_3$ in H_2O. Although the chromium ion experiences an environment of D_3 symmetry in the complex $Cr(bpy)_3^{3+}$, it is convenient for the present work to discuss the relevant part of the electronic energy level diagram in terms of the transition-metal ion experiencing octahedral symmetry (see Fig. 1). It is well known that population of the ^2E state of $Cr(bpy)_3^{3+}$ can be achieved by pumping in the $^4T_2$ band system. This because (i) the transition $^4T_2 \rightarrow {}^4A_2$ has a low probability,[3] (ii) the intersystem crossing $^4T_2 \rightarrow {}^2E$ is fast and highly efficient, and (iii) the lifetime of the ^2E state is long ($\tau_E = 63$ μs).[1] See also Fig. 2.

In order to study spectroscopic transitions of $^2E:Cr(bpy)_3^{3+}$, it is important to know how many molecules which were originally in their ground state $^4A_2$ have been converted into ^2E. Information concerning the degree of conversion can be obtained as explained in the following.

We denote the absorption cross section of the transition $^4T_2 \leftarrow {}^4A_2$ by σ_A. We assume that (i) the probability of the transition $^4T_2 \rightarrow {}^4A_2$ is negligibly small, and (ii) the quantum efficiency of the intersystem crossing process $^4T_2 \rightarrow {}^2E$ has a value of unity and the time involved is shorter than the lifetime (τ_T) of $^4T_2$. Furthermore, τ_E is the lifetime of the state ^2E and σ_E the absorption cross section for the transition $^2X \leftarrow {}^2E$ where ^2X refers to an unspecified higher-lying doublet state. Upon exposing $Cr(bpy)_3^{3+}$ to laser light having an incident intensity I_L and a wavelength falling in the band due to the transition $^4T_2 \leftarrow {}^4A_2$, we find that the attenuation of the laser radiation due to either ground ($^4A_2$) or excited state (^2E) absorption processes, is given, respectively, by:

[a)]Research supported by the Natural Sciences and Engineering Research Council of Canada.

 0021-9606/80/140688-09$01.00

$$\left(\frac{dI_L}{dx}\right)_A = -\sigma_A[N-n(x)]I_L(x) \quad (1)$$

and

$$\left(\frac{dI_L}{dx}\right)_E = -\sigma_E n(x) I_L(x) \ . \quad (2)$$

Here $n(x)$ is the density of centers in the (metastable) state ^2E at a depth x inside the absorption cell, $I_L(x)$ is the intensity at x, and N is the number of absorbing centers per unit volume. The total attenuation of the laser beam equals the sum of $(dI_L/dx)_A$ and $(dI_L/dx)_E$, and it is seen that $n(x)$ increases upon absorption of photons $^4A_2$. Under cw illumination conditions, an equilibrium value of $n(x)$ is reached at some time t where $t \gg \tau_E$. The rate of change of $n(x)$ with time is given by:

$$\frac{dn(x)}{dt} = -\frac{1}{\phi}\left(\frac{dI_L}{dx}\right)_A - \frac{n(x)}{\tau_E} \ , \quad (3)$$

where ϕ is the cross section of the laser beam (ϕ is assumed to be independent of x and the intensity profile across the beam is taken to be rectangular). The steady state condition $dn(x)/dt = 0$ gives $n(x)$ as a function of $(dI_L/dx)_A$ which, substituted in (1) and (2) followed by integration over x from $x=0$ to 1 (the length of the absorption cell) yields the result:

$$I_L(l) = I_L(0)\frac{[1+(\sigma_E\tau_E/\phi)I_L(l)]}{[1+(\sigma_E\tau_E/\phi)I_L(0)]^{(\sigma_E-\sigma_A)/\sigma_E}} e^{-\sigma_A N l} \ . \quad (4)$$

The power density is defined by $I_L(0)/\phi$, and if $I_L(0)/\phi \to 0$, Eq. (4) reduces to

$$I_L(l) = I_L(0)e^{-\sigma_A N l} \ , \quad (5)$$

while the extreme condition $I_L(0)/\phi \to \infty$ yields

$$I_L(l) = I_L(0)e^{-\sigma_E N l} \ . \quad (6)$$

Equation (4) can be tested by plotting $T = I_L(l)/I_L(0)$ as a function of $I_L(0)$. Measurement of T for low light levels yield a value for σ_A. For extremely high light levels, Eq. (6) is applicable and a value of σ_E may be computed. However, from a practical point of view the observation of the transition $^2X - {}^2E$ depends on a number of factors which are not directly reflected in the above equation. Of paramount importance is $N(\tau_E)$, which represents the number of photons per lifetime τ_E in the irradiated volume, with respect to the number of molecules occupying the same volume. For instance, for a power level of 40 mW at 457.9 nm, the irradiated area is exposed to $\sim 10^{17}$ photons per second. Having a 10^{-3} M solution of the chromium complex, we calculate the number of molecules to be $\sim 10^{17}$, and the irradiated area is a cylinder with $l = 1$ cm and $\phi \approx 0.10$ cm^2. Given the lifetime $\tau_E = 30$ μs of the present sample (not deoxygenated) one ob-

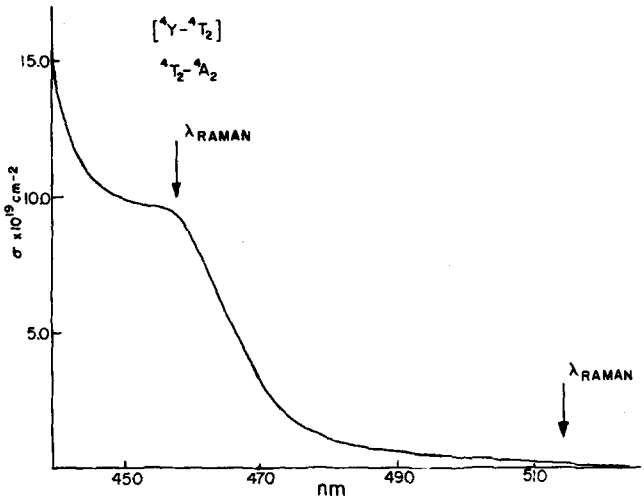

FIG. 2. Part of the absorption spectrum of the complex tris(2,2'-bipyridine)Cr(III) in H_2O. The assignment of some of the bands are shown together with the wavelengths used to excite Raman transitions of vibrational levels in $^4A_2$, ^2E, and $^4T_2$: $Cr(bpy)_3^{3+}$.

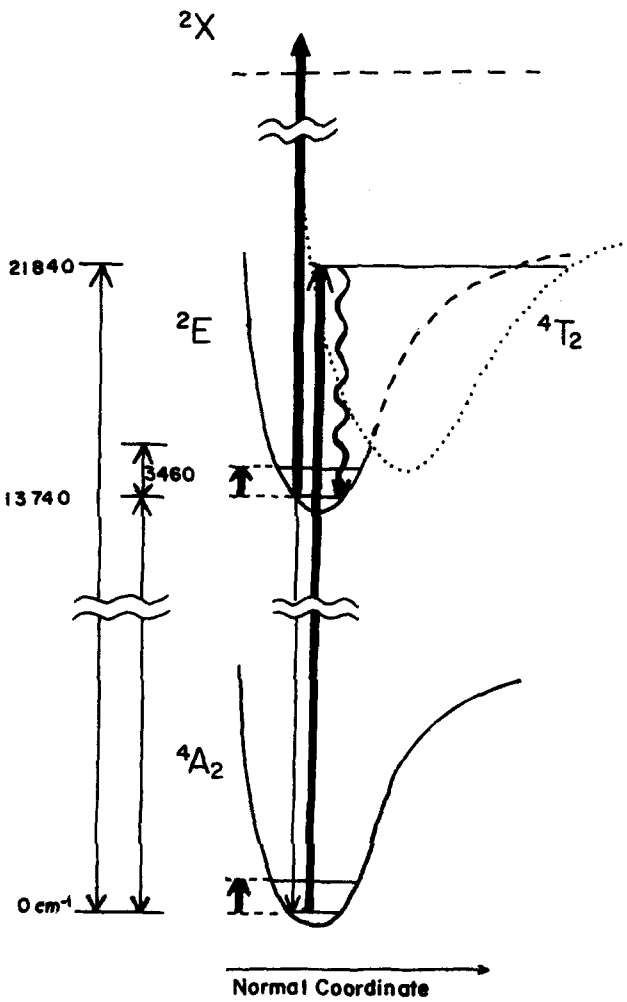

FIG. 1. Part of the energy level diagram of $Cr(bpy)_3^{3+}$ appropriate to the present studies. Shown are the $^4T_2 \leftarrow {}^4A_2$ and $^2X - {}^2E$ absorption processes at 457.9 nm with cross sections, respectively, of $\sigma_A = 8.88\times10^{-19}$ cm^2 and $\sigma_E = 6.29\times10^{-19}$ cm^2. The lifetime $\tau_{^2E} = 63$ μs and due to the small number of photons $N(\tau_{^4T_2})$ as compared to $N(\tau_{^2E})$ per number of molecules for experiments with cw fixed frequency lasers ($\sim$ 50 mW at 457.9 nm), population of ^2E (but not of $^4T_2$) occurs via the intersystem crossing process $^4T_2 \to {}^2E$. Vibrational Raman scattering can only be induced from the lowest level of the ^2E electronic surface because the intersystem crossing process is too fast (ps, level) and the time evolution of the degree of population of the upper vibrational levels of $^2E(^4T_2)$ cannot be probed with the radiation of cw fixed frequency laser ($\lambda = 457.9$ nm) pperating at the $\sim$ 100 mW power level.

tains $N(\tau_E) \approx 10^{13}$. It is obvious that even if all photons were absorbed total conversion would not be achieved. This is borne out by experiment. Shown in Fig. 3 is the value of the transmission (T) of the aqueous solution of the complex as function of laser power. The value of T is independent of $I_L(0)$ in the case where the laser beam is not focused. If focusing of the laser radiation takes place through a lens with $f = 10$ cm, then the irradiate volumes amount to $\sim 10^{-6}$ cm^3 in which there are $\sim 10^{12}$ molecules. Hence the number of molecules is approximately equal to $N(\tau_E)$ and some population of ^2E can take place. That this is actually the case is shown in Fig. 3, where it can be seen that the transmission increases and approaches a constant value.

If no absorption from ^2E occurs, then $T \to 1.0$ for large values of $I_L(0)$. However, note that a deviation of the value $T = 1$ can also be brought about if the conditions regarding the probability of the processes $^2T_2 \to {}^4A_2$ and $^4T_2 \to {}^2E$ (see above) are not met. In this case other cycles play a role, and although it appears that population of the ^2E state takes place, full bleaching of $^4A_2$ has not taken place. Only if simultaneous measurements are made of spectroscopic processes from $^4A_2$ and ^2E during the optical pumping process can conclusions be drawn to what degree $^4A_2$ is depopulated and ^2E populated. In this case, the other cycles can be neglected. A lower limiting value of $\sigma_E = 6.29 \times 10^{-19}$ cm^2 can be computed, while $\sigma_A = 8.88 \times 10^{-19}$ cm^2.

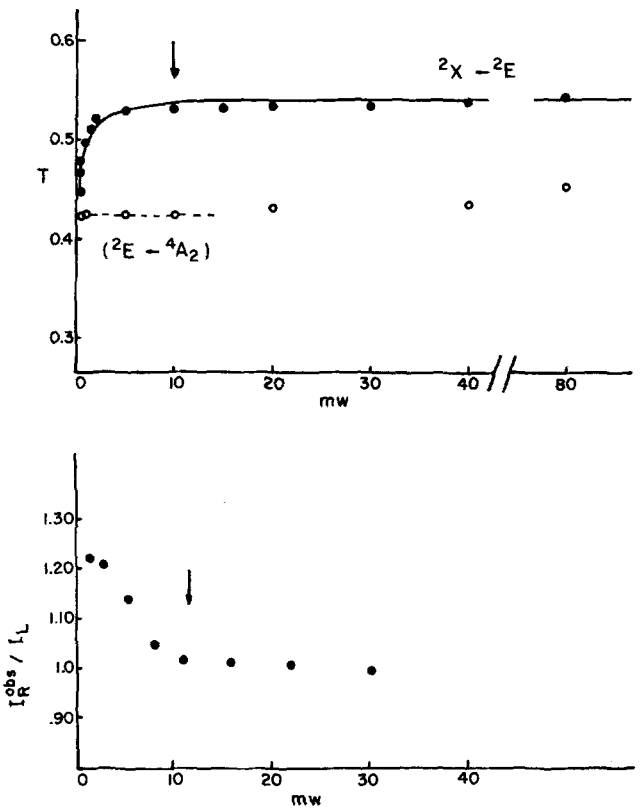

FIG. 3. Top: Transmission of a 3.2×10^{-3} molar solution of the complex $Cr(bpy)_3(ClO_4)_3$ in H_2O as function of the power of a fixed frequency cw laser ($\lambda = 457.9$ nm). The horizontal dashed line represent the behavior of the transmission due to $^4T_2 \to {}^4A_1$, but because energy is transferred into ^2E, this is indicated by $(^2E \to {}^4A_2)$. Upon focusing the laser beam into the solution, the transmission increases and appears to reach an a asymptotic value. Population of the $^4A_2$ ground state decreases and a $^2X \to {}^2E$ transition gains intensity (also at 457.9 nm). The solid curve is computed by employing Eq. (4) and the following values of the parameters: $\sigma_A = 8.88 \times 10^{-19}$ cm^2, $\sigma_E = 6.29 \times 10^{-19}$ cm^2, $l = 5$ mm, and $\phi = 5.3 \times 10^{-8}$ cm^2. The latter is smaller than computed if a beam of 3 mm is focused with a lens of $f = 10$ cm and the difference could be due to self-focusing effects (Ref. 20). Bottom: Ratio of I_R^{obs}/I_l as function of the laser power at 457.9 nm. I_{obs}^R is the integrated intensity (arbitrary units) of a band at ~ 1040 cm^{-1}. The curve follows that of the behavior of T and the total intensity of the Raman band at values of $I_L > 10$ mW is mainly due to scattering of ^2E rather than that of the mode in $^4A_2$.

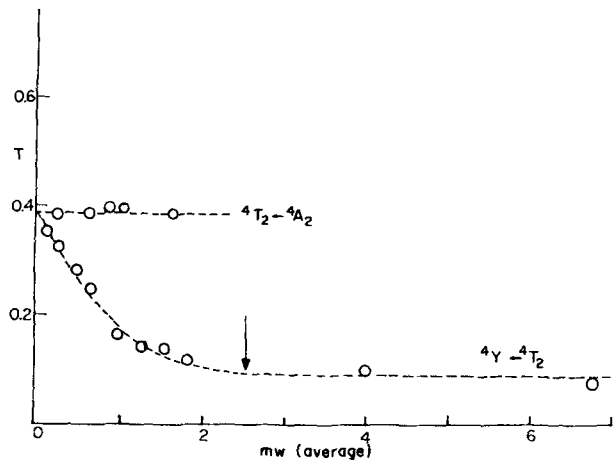

FIG. 4. Transmission of the sample as function of the power of the pulsed laser at 457.9 nm. The horizontal curve is due to $^4T_2 \to {}^4A_2$ transitions but upon focusing of the laser light, transitions of $^4Y < {}^4T_2$ become more abundant due to population of $^4T_2$ levels. The cross section of these transitions $\sigma_{^4T_2} \approx 2.56 \times 10^{-18}$ cm^2. The decrease in T and its constant value for $I_L > 2.5$ mW (average power) is in the present analysis not interpreted in terms of bleaching of $^4A_2$. Rather, within the time frame of the duration of the laser pulse, the majority of the $Cr(bpy)_3^{3+}$ molecules are considered to be in the $^4T_2$ excited state and spectroscopic processes (like Raman or other transitions) associated with $^4A_2$ cannot be detected anymore.

In Fig. 4 we show the results of measurements of T of the same sample but now with radiation of a pulsed laser (at $\lambda = 457.9$ nm). The duration of the pulse is ~ 4 ns with a peak power of $\sim 10^5$ W which corresponds to $\sim 10^{15}$ photons/pulse. The value of T for the unfocused beam in the pulsed experiments does not differ from the value measured with the cw laser; however, this is not the case if a comparison is made of the value of T for the focused beams. The transmission decreases upon an increase in $I_L(0)$ in the former, but increases in the latter case before reaching a constant value. Detailed measurements of T for low values of $I_L(0)$ of the pulsed dye laser shows that T does *not* increase to the value $T = 0.55$ before experiencing the rather pronounced decrease to $T = 0.09$. This shows that population of ^2E does not take place at some low light level. Rather, another (and competitive with regard to the $^4T_2$-^2E intersystem crossing) process takes place. This process must involve $^4T_2$ (Fig. 5). The fact that ^2E does not get populated in the pulsed experiment is in agreement with the following experimental observation. Whereas

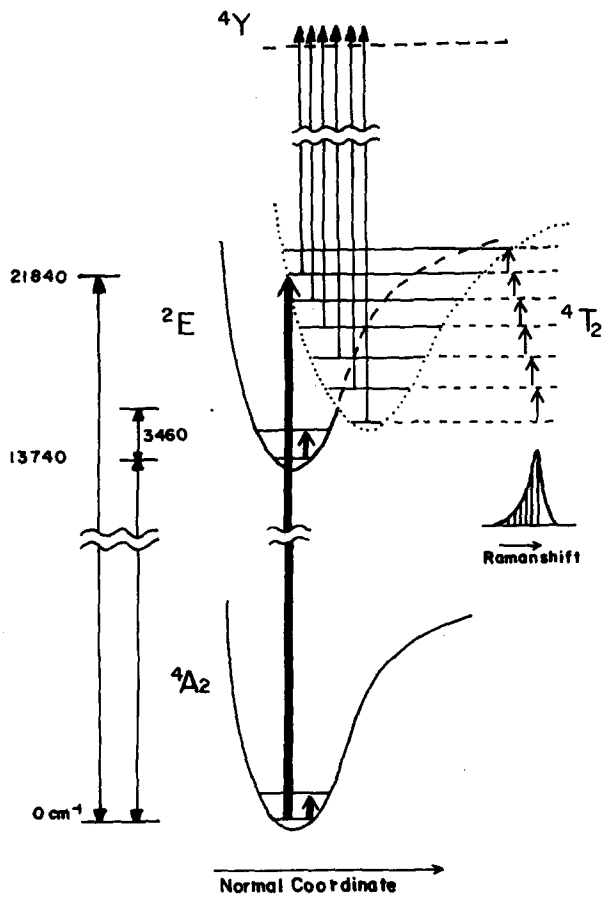

FIG. 5. Spectroscopic processes in ground and excited states of $Cr(opy)_3^{3+}$ in the system are exposed to radiation of a pulsed laser at 457.9 nm. The number of photons per lifetime $\tau_{^4T_2}$ is now of the same order of magnitude as the number of molecules. Population of vibrational levels of the $^4T_2$ electronic surface takes place, and the time evolution of the population can be probed via (i) an observation of ^4Y-$^4T_2$ transitions or (ii) of Raman transitions from successive vibrational levels. Due to a decreasing energy difference of successive vibrational levels by increasing value of the vibrational quantum number, one predicts an asymmetry in the band contour of the vibrational Raman band. Intersystem crossing to ^2E is considerably reduced because, after population of levels in $^4T_2$ occurs, subsequent absorptions of photons (with $\lambda = 457.9$ nm) due to $^4Y \leftarrow {}^4T_2$ transitions (with a rather large cross section) take place during the ~4 ns duration of the laser pulse.

strong phosphorescence due to $^4A_2 \leftarrow {}^2E$ is excited under cw irradiation, the phosphorescence process has a nearly vanishing intensity if the complex is exposed to the focused radiation at $\lambda = 457.9$ nm of the pulsed laser. The intensity of the said phosphorescence is only slightly increased if the intensity of the pulsed laser is reduced, indicating that some $^4T_2 \rightarrow {}^2E$ intersystem crossing process takes place. The behavior of the transmission in the pulsed situation (focused case) is not due to the presence of a photochemically induced chemical species. This and other aspects follow from a comparison of the Raman spectrum taken during the duration of the pulse (see Sec. III). The decrease of T displayed in Fig. 4 seems to be a result of the occurrence of population of the $^4T_2$ state. Subsequent absorption of photons with $\lambda = 457.9$ nm seems to be due to a $^4Y \leftarrow {}^4T_2$ transition.

Photochemical evidence points to the fact[16] that the saddle point of $^4T_2$ and ^2E electronic surfaces is at ~17 200 cm^{-1}, while ^2E is ~13 740 cm^{-1} above the ground state. It thus appears that the radiation at 457.9 nm is in resonance with vibrational states having a large v of normal modes in $^4T_2$. The energy pumped in these levels reaches levels with smaller v values via a rapid vibrational relaxation process (see Fig. 5 and Sec. III for details), and population of the levels in the bottom of the potential well takes place. Population of these low-lying vibrational states or even a saturation effect is apparently achieved (see Fig. 5) because, in effect, we deal here with a pseudo three level system (ground state, short-lived vibrational states in the top of the surface, and longer-lived vibrational states in the bottom). The $^4Y \leftarrow {}^4T_2$ absorption transitions (induced with $\lambda = 457.9$ nm) can, in the pulsed case, originate in the populated levels of the $^4T_2$ electronic surface, and in fact an apparent resonance two-photon absorption process takes place. The levels in the bottom of the $^4T_2$ potential surface are for all practical purposes not populated in the cw case because the number of photons per lifetime $\tau_{^4T_2} \approx 10$ ps (see the following) is down by ~seven orders of magnitude if compared to the number of photons per $\tau_{^4T_2}$ delivered by the pulsed laser. Hence the occurrence of a $^4T_2 \rightarrow {}^2E$ intersystem crossing in the cw case. The $^4Y \leftarrow {}^4T_2$ transitions (pulsed case) can be probed in the region of $450 > \lambda_{\text{laser}}^{\text{pulsed}} > 400$ nm.

An identical number of molecules is exposed to the radiation of pulsed and cw lasers because the same lens was employed for focusing purposes. Furthermore, the same absorption process at 457.9 nm (that due to $^4T_2 \leftarrow {}^4A_2$) is responsible for population of ^2E (cw laser) and $^4T_2$ (pulsed laser). We conclude that saturation effect does occur because the value of the transmission appears to have reached a constant value for certain values of $I_L(0)$ (cw) and $I_L(0)$ (pulse). At the point of saturation $I_L(0)$ (cw) = 10 mW (which corresponds to 2.3×10^{16} photons/s), while $I_L(0)$ (pulsed) = 2.5 mW (which corresponds to 2.1×10^{14} photons/pulse), and we find (see Sec. II) that $N(\tau_{^2E}) = N(\tau_{^4T_2})$. The lifetime of the ^2E state was determined to be $\tau_{^2E} = 30 \times 10^{-6}$ s, and we compute $\tau_{^4T_2} \approx 10$ ps assuming that (i) the $^4T_2 \rightarrow {}^2E$ intersystem process has a quantum efficiency of unity and (ii) the probability of the $^4A_2 \leftarrow {}^4T_2$ fluorescence process is small.

III. OPTICAL PUMPED EXCITED STATE RAMAN TRANSITIONS OF ^2E AND $^4T_2$

A. Theoretical remarks

It is clear from the transmission studies of the $Cr(bpy)^{3+}$ complex in water that not all photons are absorbed. For instance (see Fig. 3), if the complex is exposed to 50 mW of the cw laser radiation, for the experiment where the beam is not focused, at least 20 mW at 457.9 nm is available for Raman probing. The power level even increases in the case where the beam is focused into the cell. This suggests that it is convenient to study Raman transitions of an excited state with the radiation of a single laser, part being used for pumping purposes and the rest for Raman probing.

In the situation where population of excited state i occurs, the observed overall intensity $(I_R^{obs})_q$ of a Raman band due to a normal mode q in this state i is given by

$$(I_R^{obs})_q = \sum_i \{n_i I^i(q)\} . \quad (7)$$

and

$$\frac{(I_R^{obs})_q}{I_L} = \sum_i \{n_i Q^i(q)\} , \quad (8)$$

where I_L is the laser intensity available for Raman probing, n_i is the population of the state i so that $\sum_i n_i = 1$. The cross sections $Q^i(q)$ for scattering of the normal mode is then given by

$$Q^i(q) = \frac{2^7\pi^5}{3^2C^4}(\nu_L - \omega_q^i)^4 \sum_{\rho\sigma} \left| \left(\frac{d\alpha_{\rho\sigma}^i}{dq} \right) \right|^2 . \quad (9)$$

Here ν_L is the frequency of the laser radiation, ω_q^i that of the normal mode q in i, and $\alpha_{\rho\sigma}^i$ the polarizability tensor for q^i. We note that all $Q^i(q)$ are in principle different for all i because the denominators of the well known expression for $\alpha_{\rho\sigma}$ are not equal.

In the situation where population of only one excited state occurs, the observed overall intensity $(I_R^{obs})_q$ of a vibrational Raman band for the mode q in the ground state G and an excited state E, is given by

$$(I_R^{obs})_q = n_G I_G(q) + n_E I_E(q) , \quad (10)$$

$$(I_R^{obs})_q / I_L = n_G Q^G(q) + n_E Q^E(q) . \quad (11)$$

$Q(q)^G$ is not necessarily equal to $Q^E(q)$ [see Eq. (9)]. Also, $n_E + n_G = 1$ and $\omega^E(q)$, $\omega^G(q)$ are the frequencies of vibration in E and G, respectively. It is clear from Eq. (11) that if $Q^G(q) = Q^E(q)$, the ratio $I_R^{obs}/I_L = \text{const}$, and one is *not* in a position to separate the Raman scattering in the excited state from that in the ground state if $\omega^E(q) = \omega^G(9)$. However, by virtue of the fact that the optical pump, which at the same time serves as Raman probe for the ground state transition, is in resonance with an absorption band of the system, a resonance Raman effect governs the intensity of transitions from the ground state. A similar but different resonance Raman process may also occur in the excited state. Consequently [apart from the considerations made with regard to the $Q^i(q)$ of Eq. (9)], $Q^G(q) \neq Q^E(q)$, which in turn suggests that $(I_R^{obs})_q$ is *not* linear in I_L.

If the potential surfaces of the electronic states G and E are not equal, the Raman transitions become separated because $\omega^E(q) \neq \omega^G(q)$. The intensity of the normal mode q in the state E becomes $(I_R^{obs})_q^E \propto I_L^2$ and $(I_R^{obs})_q^G$ is not dependent on I_L as long as saturation population of E is not reached. The assignment of an excited state vibrational Raman process, in terms of frequency and/or intensity, is then straightforward.

Probably the most important feature of excited state Raman spectroscopy is its inherent resolution which is extraordinary in comparison with the inherent broad spectral features obtained with conventional absorption methods. In the latter, many different and complicated processes such as intermolecular interactions or spectral coincidences of vibronic sidebands of two close lying electronic excited states are responsible for the spectral features. Such effects are either nonexistent or affect to a much lesser extent the excited state Raman spectrum.

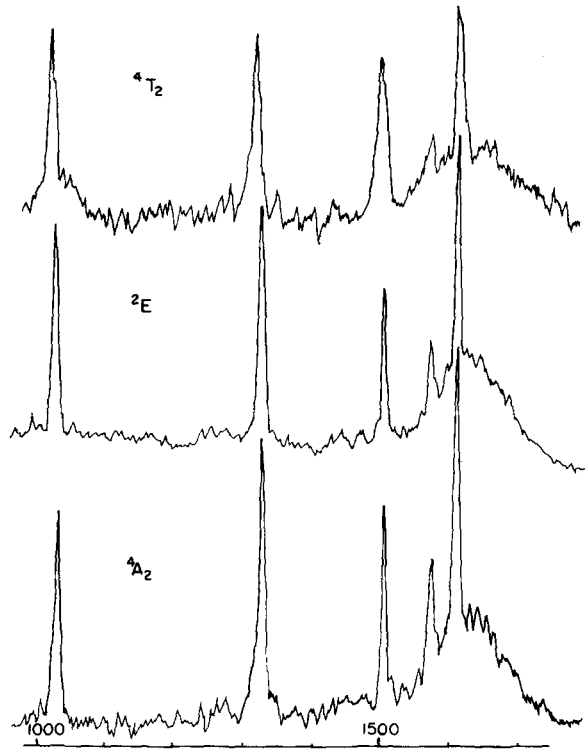

FIG. 6. Part of the Raman spectrum of $Cr(bpy)_3^{3+}$ recorded with the pulsed laser apparatus. The Raman shifts are due to normal modes involving motions of the atoms of the bipyridine rings. The top spectrum is that with the laser radiation > 2.5 mV (average) focused into the cell, consequently (see Fig. 5), Raman spectra are induced from $^4T_2$ only. The lower spectrum is that with the beam unfocused (horizontal line in Fig. 5) and represents light scattering from $^4A_2$ only.

B. Experimental results ^2E : $Cr(bpy)_3^{3+}$

Some parts of the Raman spectrum of $Cr(bpy)_3^{3+}$ excited with the 457.9 nm of a cw laser are shown in Figs. 6 and 7, and relevant data on the position, assignment, etc. of the bands is given in Table I. The spectra were taken from the cell which is also used in the absorption measurements (Sec. II), and the transmission of the sample was in fact monitored while the light scattering spectrum was recorded. In an earlier paper, the frequency of the Raman shifts of $Cr(bpy)_3^{3+}$ in the spectral range of 1000–1700 cm^{-1} was discussed, and we mentioned in passing[13] that the positions of the Raman transitions do change for spectra recorded with the laser beam focused or not focused inside the cell. The Raman bands which are of interest here are at 1041, 1326, 1505, 1573, and 1610 cm^{-1}. Those due to metal-ligand vibrations occur below 600 cm^{-1}, are weak, and have such a large bandwidth that changes could not be detected. Their assignment in terms of the irreducible representations of the group D_3 (see also Table I) is based on a normal coordinate analysis of the infrared spectrum of 2,2'-bipyridine performed by Strukl and Walter.[17] Additional spectral studies were carried out by Castellucei and Angeloni[18] for the non-complexed

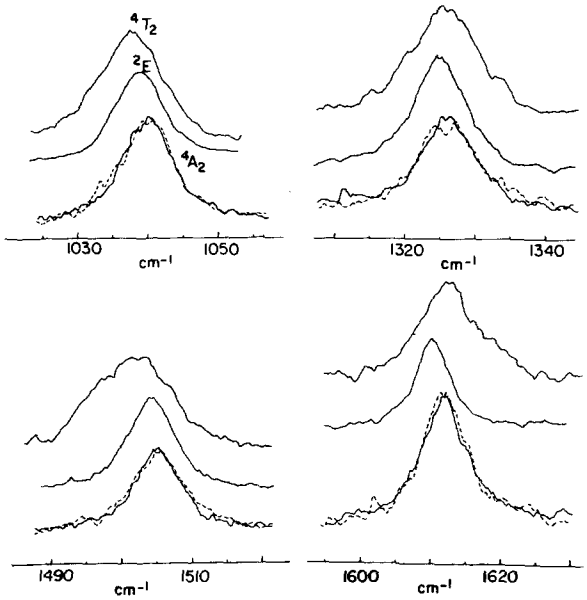

FIG. 7. Comparison of the band contours of a Raman effect of $^4T_2$ and $^4A_2$: $Cr(bpy)_3(ClO_4)$ in H_2O.

molecule in its transconfiguration in the liquid and solid (single-crystal) state. The bipyridine ligands of the complex discussed in the present work have the *cis* configuration. However, the observed frequencies for vibrations of these ligands are very close to those of the free ligand, and as a result we assume that a correlation can be made for similar modes of vibration of the free molecule and complexed ligand. This assumption is supported by the fact that because all modes of Table I belong to the totally symmetric species of the group D_3 their depolarization ratio should be $<\frac{3}{4}$, which is in agreement with our experimental findings. Presently, we discuss the intensity changes of Raman bands as function of the power density of the laser beam in the two cases (defocused and focused). In order to do so, we have to know the geometrical relationship of intensities for Raman scattering in the situation where the beam is focused and not focused in the cell. This relationship depends on the geometry of the collection optics of the light scattering apparatus and on the focal length of the lens employed to focus the beam inside the cell. The results of intensity measurements of the Raman shift of 1040 cm^{-1} are shown in Fig. 3 and the geometrical factor has been introduced to relate the intensities in the two cases. We note that there exists a nearly one-to-one relationship between the change in the cross section of this Raman transition and the change in transition characteristics at $\lambda = 457.9$ nm of the same sample (see Fig. 3). At power levels of ~20 mW saturation population of the ^2E state of $Cr(bpy)_3^{3+}$ seems to have occurred and the cross section for the intensity of the Raman shift remains constant. This is in agreement with Eq. (8), because for apparent population saturation of ^2E we find that $I_R^{obs}/I_L = N_T Q^E(q)$. However, for the experimental situation where the beam is not focused and conditions of population saturation are not met, according to Eq. (1) $I_R^{obs}/I_L = N_T Q^G(q)$, which relationship is seen to be in perfect agreement with the intensity measurements (Fig. 3).

The experimental data mentioned above are interpreed in terms of apparent saturation population of the excited state which should not be confused with bleaching of $^4A_2$ because the direct $^4A_2 \rightarrow {}^4T_2$ fluorescence process may be present and the efficiency of the intersystem crossing process $^4T_2 \rightarrow {}^2E$ may not be 100%.[1] Such processes which may also be characterized by the lifetimes τ_{F1} and τ_{ISC}, respectively, can only play a role if $N(\tau_{F1})$ and/or $N(\tau_{ISC})$ are of the same order of magnitude (or larger) as the number of molecules in the irradiated area. These lifetimes however are expected to be in the picosecond range[1]; therefore neither processes are important with respect to measurements carried out with the power level of the cw lasers used in the present experiment. It is, however, clear from the behavior of the transmission T and I_R^{obs}/I_L as function of I_L that within experimental limits conditions exists which reflect a

TABLE I. Frequencies and assignments of some of the more prominant Raman's due to normal modes of $Cr(bpy)_3^{3+}$ modes of $Cr(bpy)_3^{3+}$ in ground ($^4A_2$) and excited states ^2E and $^4T_2$.

		1041 cm^{-1}	1326 cm^{-1}	1505 cm^{-1}	1573 cm^{-1}	1610 cm^{-1}
Defocused ($^4A_2$)	FWHM (cm^{-1})	8.5±0.5	8.8±0.5	8.0±0.5	9.5±1.0	8.0±0.5
cw focused (^2E)	Shifts from Def. case (cm^{-1})	−1.2	−1.2	−0.8	−1.5	−2.0
	FWHM (cm^{-1})	8.5±0.5	8.6±0.5	8.0±0.5	7.5±1.0	6.5±0.5
Pulsed focused	Shifts from Def. case (cm^{-1})	−2.5	−0.6	−2.8	−2.0	0.0
($^4T_2$)	FWHM (cm^{-1})	10.0±0.5	11.0±0.5	13.5±0.5	11.5±1.0	9.5±0.5
Symmetry species in D_3		A_1	A_1	A_1	A_1	A_1
$\rho_{^4A_2}$; bpy		0.2~0.4	0.2~0.4	0.2~0.4	0.2~0.4	0.2~0.4
Assignment		ring-ring structure	CH deformation	CH deformation	in plane ring	in plane ring

situation of a *de facto* population inversion of ^2E (or $^4T_2$) versus $^4A_2$. In other words, the recorded spectra could contain scattering due to normal modes of the ground state; however, the contribution to the observed intensity profile is not detectable. None of the observed Raman bands exhibit a profile showing asymmetry[13] that could be interpreted in terms of the presence of scattering from normal modes in the ground state. A summary of the results of ^2E: $Cr(bpy)_3^{3+}$ in comparison with corresponding data for $^4A_2 : Cr(bpy)_3^{3+}$ is given in Table I.

Based on the preceding, we assume that in all other experiments where the transmission behavior of the sample at high laser powers is similar to that encountered in the present experiments the induced Raman spectra are those associated with the optically pumped excited state. It may,, however, be worthwhile to note here that saturation population effects of an excited state can only be realized in a three (or more) level system of which the present molecular complex is a good example. For a two level system saturation population cannot be achieved, and the Raman spectrum can at best be composed of equal contributions of scattering in ground and excited states, although of course the former is always affected by resonance effects.

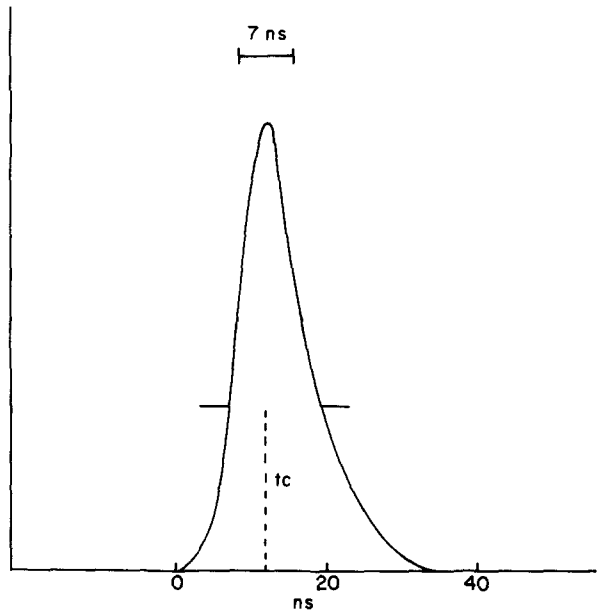

FIG. 8. Pulse shape due to Raman scattered light of the shift at ~1040 cm^{-1}.

C. Experimental results $^4T_2 : Cr(bpy)_3^{3+}$

Part of the Raman spectrum of the chromium bipyridine complex in water excited with 3.2 ns pulse (>100 kW peak power) of a tunable dye laser is also shown in Fig. 6 and spectral details of some of the bands are displayed in Fig. 7. A description of the pulsed laser Raman spectrometer will be published elsewhere. Of interest here is the fact that the performance of this system, in terms of signal-to-noise ratios, is about the same as that encountered with conventional cw laser Raman spectrometers operating in the 100 mW power range (from 457.9–514.5 nm). The pulsed system, however, has the capacity to display the Raman scattered light pulses in real time, a feature which is nonexistent in conventional laser Raman spectrometer. The spectra obtained with the pulsed laser spectrometer were also obtained from the cell used in the absorption studies, and in fact the transmission of the sample was monitored during the pulsed laser Raman studies. The average laser power was such that the transmission of the sample was $T = 0.09$ (see Fig. 4), indicating that the experimental results are those for $^4T_2 : Cr(bpy)_3^{3+}$ rather than $^4A_2 : Cr(bpy)_3^{3+}$, but vibrational scattering from the latter could be recorded by reducing the laser power level. A comparison of the spectra displayed in Fig. 6 shows that the overall aspects are not all that different. However, although only small differences appear to exist for intensity and band center frequencies of corresponding Raman shifts for $^4A_2$ and $^2E : Cr(bpy)_3^{3+}$, these differences are more pronounced for $^4A_2$ and $^4T_2 : Cr(bpy)_3^{3+}$. See also Table I. The cross sections of the $^4Y \leftarrow {}^4T_2$, $^4T_2 \leftarrow {}^4A_2$, and $^2X \leftarrow {}^2E$ transitions are, respectively, $\sigma_{^4T_2} = 2.56\times10^{-18}$ cm^2, $\sigma_{^4A_2} = 8.88\times10^{-19}$ cm^2, and $\sigma_{^2E} = 6.29\times10^{-19}$ cm^2. Consequently, resonance Raman effects could in principle affect the intensity pattern of modes of $^4T_2 : Cr(bpy)_3^{3+}$ to a different extent than those of ^2E and $^4A_2 : Cr(bpy)_3^{3+}$. The experimental results are not in disagreement with this prediction, because the Raman intensity of the various bands relative to the one with a shift of ~1040 cm^{-1} in the $^4T_2$ spectrum is not quite the same as a similarly calculated intensity pattern for the $^4A_2$ spectrum. Such a comparison of the ^2E and $^4A_2$ spectensity patterns, however, yields even smaller differences.

The spectra obtained with the pulsed laser are just as clean as those recorded with the cw laser at 457.9 nm. Photochemical processes during the pulsed laser experiments do take place,[2] because the transmission of the samples changes if exposed for longer periods than the duration of the light scattering measurement to the >100 kW peak power laser pulses. Scattering of the photochemical products is not observed and it appears that fragments are formed after the duration of the laser flash (3.2 ns), at which time the Raman probe has left the sample cell. The variation in changes in the shifts of corresponding Raman band (see Table I) of ground and ^2E or $^4T_2$ excited states of $Cr(bpy)_3^{3+}$ are most probably related to the fact that the $^4T_2$ orbital, contrary to the one for ^2E of the chromium complex, contains antibonding character. A comparison of band contours of various Raman transitions displayed in Fig. 7 reveals that the Raman bands of $^4T_2 : Cr(bpy)_3^{3+}$ centered around ~1503, 1572, and 1040 cm^{-1} show broadening towards lower energy which gives rise to the asymmetric based contours. According to the energy level diagram for $Cr(bpy)_3^{3+}$, we find that the radiation of the pulsed laser at $\lambda = 457.9$ nm is in resonance with the energy of vibrational states with $v > 5$ of those normal modes having a fundamental frequency in the range of 1000–1600 cm^{-1}. Given the rapid rise time (t_p) of the light pulse of ~2 ns, it is conceivable that—apart from populating the levels in the bottom of the $^4T_2$ surface which have a lifetime of ~10 ps—population of the higher vibrational states takes place. Thus the degree of population depends on the ra ratio of the value of the vibrational relaxation time t_{VR}

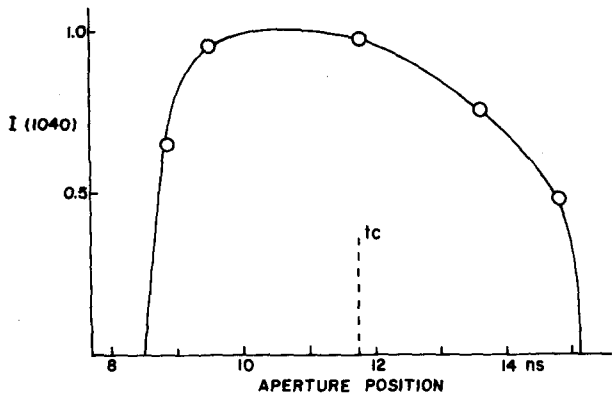

FIG. 9. Integrated intensity of the Raman band at ~1040 cm^{-1} as a function of the position of the aperture duration (gate) of the boxcar in real time. The curve is not symmetric around $t=t_c$ (see also Fig. 8) and the additional intensity for $t<t_c$ is attributed to Raman transitions originating in the top of the $^4T_2$ electronic surface. See also Fig. 5. The time evolution of the population of these states is of such a nature that it can be Raman probed during the rise time of the laser pulse. The shorter the time evolution process, in comparison to this rise time, the more symmetric the intensity curve should become.

and t_p, and the population of the various vibrational levels is dynamic. The intensity profile of the laser pulse in real time is Gaussian, and we deduce that during the rise time of this pulse, Raman processes of the populated levels may be probed in the top of the potential well. These processes become more difficult to detect during the decay time of the laser pulse, because during the decay time the population characteristics of the vibrational levels changes in favor of population of levels situated in the bottom of the potential surface. Figure 8 shows the form of the Raman light pulse in real time as obtained with a boxcar integrator. The full width at half-maximum (FWHM) of the laser pulse itself is 3.2 ns but the instrument (aperture duration of the gate of ~7 ns) enlarges this value to ~8 ns. By adjusting the aperture of the boxcar in real time the effect of the leading edge, center, and trailing end of the pulse on the overall intensity of a Raman band can be studied. The observed Raman intensity I_R^{obs} of the full band as function of this position of the aperture in real time is shown in Fig. 9, and we note an asymmetric behavior of I_R^{obs} around $t=t_c$. Realizing that the intensity of a vibrational Raman transition I_v from the vth level[19] is related to the intensity of the transition (I_0) from $v=0$ by the expression $I_v=(v+1)I_0$, we conclude that the asymmetric behavior is in fact due to a greater contribution to the intensity of transitions of levels in the top of the potential surface during the rise time of the pulse (as compared to their contribution to the overall intensity during the decay time of the pulse). The asymmetry in the Raman band contours towards lower energy (Fig. 7) is in agreement with the preceding because this asymmetry is a result of anharmonicity effects which produce a decreasing energy gap of successive vibrational states upon an increase of the values v. The larger the anharmonicity, the greater the asymmetry in the band contours (frequency spectrum).

We conclude this section with the remark that in order to obtain a distinct Raman spectrum of normal modes in an electronic excited state, it is paramount to move away from a simple two level system (the ground and electronic excited state). Only in a three (or more) level system is it possible to reach conditions of population inversion of the electronic excited state. These many level systems imply energy transfer, which in nearly all cases involve vibrational relaxation mechanisms. The shorter the lifetime of the excited state, the shorter the duration of the light pulse must be in order to achieve population inversion, but the more likely spectral interferences due to the vibrational relaxation process are. The present chromium complex is a good example. Whereas the lifetime of the ^2E state is long (and even a cw laser can be used to pump and Raman probe), the effect of intersystem crossing (which is vibrational in nature) does not show up (the widths of Raman bands of ^2E and $^4A_2$: $Cr(bpy)_3^{3+}$ are the same). However, the lifetime of $^4T_2$ is much shorter and vibrational relaxation effects do influence the Raman bands, particularly their width. The shorter such lifetimes, the more pronounced the role these broadening effects are apt to play in vibrational Raman spectra induced from electronic excited states having even shorter lifetimes, for example, $\tau_{^4T_2} \approx 10$ ps for $Cr(bpy)_3^{3+}$.

ACKNOWLEDGMENTS

The authors wish to thank Dr. Langford and Dr. Sasseville for discussions and providing them with samples. One of us (J.A.K.) gratefully acknowledges support from the Natural Sciences and Engineering Research Council of Canada which enabled us to carry out the pulsed laser Raman studies.

[1]M. Maestri, F. Bolletta, L. Moggi, V. Balzani, M. S. Henry, and M. Z. Hoffman, J. Am. Chem. Soc. **100**, 2694 (1978). See also F. Boletta, M. Maestri, L. Moggi, and V. Balzani, J. Chem. Soc. Chem. Commun. 901 (1975).
[2]M. Maestri, F. Bolletta, N. Serpone, L. Moggi, and V. Balzani, Inorg. Chem. **15**, 2048 (1976).
[3]F. Bolletta, M. Maestri, and V. Balzani, J. Phys. Chem. **80**, 2499 (1976).
[4]M. S. Henry, J. Am. Chem. Soc. **99**, 6138 (1977).
[5]M. A. Jamieson, M. Serpone, and M. Maestri, Inorg. Chem. **17**, 2432 (1978).
[6]N. Serpone, M. A. Jamieson, M. S. Henry, M. Z. Hoffman, F. Bolletta, and M. Maestri, J. Am. Chem. Soc. **101**, 2907 (1979).
[7]R. Sasseville, Ph.D. thesis, Carleton University (Ottawa), 1980.
[8]L. V. Haley, B. Halperin, and J. A. Koningstein, Chem. Phys. Lett. **54**, 389 (1978).
[9]J. P. Devlin and M. G. Rockley, Chem. Phys. Lett. **56**, 608 (1978).
[10]B. Halperin and J. A. Koningstein, J. Chem. Phys. **69**, 3302 (1978).
[11]R. Wildrandt, N. H. Jensen, P. Pagsverg, A. H. Sillesen, and K. B. Hansen, Nature (London) **276**, 167 (1978).
[12]R. F. Dallinger, W. H. Woodruff, J. Am. Chem. Soc. **101**, 4391 (1979).
[13]M. Asano, D. Mongeau, D. Nicollin, R. Sasseville, and J. A. Koningstein, Chem. Phys. Lett. **65**, 293 (1979).
[14]H. Fabian, A. Lau, W. Werncke, M. Pfeiffer, K. Lenz, and

H. J. Weigmann, Kvantovaya Elektron. (Moskow) **6**(1), 72 (1979).
[15]A. Szabo, Opt. Commun. **12**, 366 (1974).
[16]C. H. Langford and R. Sasseville, Inorg. Chem. (to be published).
[17]J. S. Strukl and J. L. Walter, Spectrochim. Acta **27**, 209 (1971).
[18]E. Castellucci, L. Angeloni, N. Neto, and G. Sbrana, Chem. Phys. **43**, 365 (1979).
[19]J. A. Koningstein, *Introduction to the Theory of the Raman Effect* (D. Reidel Publishing Co., Holland, 1972).
[20]J. R. Whinnery, Acc. Chem. Res. **7**, 225 (1974).